Innovations Deserving
Exploratory Analysis Programs

IDEA

Highway IDEA Program

Developing Embedded Wireless Strain/Stress/Temperature Sensor Platform for Highway Applications

Final Report for NCHRP IDEA Project 129

Prepared by:

Kun Lian, Center for Advanced Microstructures and Devices (CAMD), Louisiana State University, Baton Rouge, Louisiana

March 2010

TRANSPORTATION RESEARCH BOARD

OF THE NATIONAL ACADEMIES

INNOVATIONS DESERVING EXPLORATORY ANALYSIS (IDEA) PROGRAMS

MANAGED BY THE TRANSPORTATION RESEARCH BOARD (TRB)

This NCHRP-IDEA investigation was completed as part of the National Cooperative Highway Research Program (NCHRP). The NCHRP-IDEA program is one of the four IDEA programs managed by the Transportation Research Board (TRB) to foster innovations in highway and intermodal surface transportation systems. The other three IDEA program areas are Transit-IDEA, which focuses on products and results for transit practice, in support of the Transit Cooperative Research Program (TCRP), Safety-IDEA, which focuses on motor carrier safety practice, in support of the Federal Motor Carrier Safety Administration and Federal Railroad Administration, and High Speed Rail-IDEA (HSR), which focuses on products and results for high speed rail practice, in support of the Federal Railroad Administration. The four IDEA program areas are integrated to promote the development and testing of nontraditional and innovative concepts, methods, and technologies for surface transportation systems.

For information on the IDEA Program contact IDEA Program, Transportation Research Board, 500 5th Street, N.W., Washington, D.C. 20001 (phone: 202/334-1461, fax: 202/334-2081, http://www.nationalacademies.org/trb/idea)

The project that is the subject of this contractor-authored report was a part of the Innovations Deserving Exploratory Analysis (IDEA) Programs, which are managed by the Transportation Research Board (TRB) with the approval of the Governing Board of the National Research Council. The members of the oversight committee that monitored the project and reviewed the report were chosen for their special competencies and with regard for appropriate balance. The views expressed in this report are those of the contractor who conducted the investigation documented in this report and do not necessarily reflect those of the Transportation Research Board, the National Research Council, or the sponsors of the IDEA Programs. This document has not been edited by TRB.

The Transportation Research Board of the National Academies, the National Research Council, and the organizations that sponsor the IDEA Programs do not endorse products or manufacturers. Trade or manufacturers' names appear herein solely because they are considered essential to the object of the investigation.

Innovations Deserving
Exploratory Analysis Programs

IDEA

Highway IDEA Program

Developing Embedded Wireless Strain/Stress/Temperature Sensor Platform for Highway Applications

Final Report for NCHRP IDEA Project 129

Prepared by:

Kun Lian, Center for Advanced Microstructures and Devices (CAMD), Louisiana State University, Baton Rouge, Louisiana

March 2010

TRANSPORTATION RESEARCH BOARD

OF THE NATIONAL ACADEMIES

The NCHRP IDEA 129 Project is jointly funded by the Louisiana Transportation Research Center (LTRC) under work order #736-99-1496.

NCHRP IDEA PROGRAM COMMITTEE

CHAIR
SANDRA Q. LARSON
IOWA DOT

MEMBERS
RICK COLLINS
Texas DOT
GARY A. FREDERICK
New York State DOT
GEORGENE GEARY
Georgia DOT
JOE MAHONEY
University of Washington
MICHAEL MILES
California DOT
JAMES M. SIME
Connecticut DOT
MICHEAL M. SPRINKEL
Virginia DOT
A KEITH TURNER
Colorado School of Mines
RICHARD WEILAND

FHWA LIAISON
DAVID KUEHN
Federal Highway Administration

TRB LIAISON
RICHARD CUNARD
Transportation Research Board

COOPERATIVE RESEARCH PROGRAM STAFF
CRAWFORD F. JENCKS
Deputy Director, Cooperative Research Programs

IDEA PROGRAMS STAFF
STEPHEN R. GODWIN
Director for Studies and Special Programs
JON M. WILLIAMS
Program Director, IDEA and Synthesis Studies
INAM JAWED
Senior Program Officer
DEMISHA WILLIAMS
Senior Program Assistant

EXPERT REVIEW PANEL
DAVE HUFT, *South Dakota Department of Transportation*
KEVIN GASPARD, *Louisiana Trans. Research Center*
MARK MARTINEZ, *Louisiana Trans. Research Center*
ZHONG WU, *Louisiana Trans. Research Center*
JEFF LAMBERT, *Louisiana Dept. of Transportation & Dev.*
ZHONGJIE ZHANG, *Louisiana Trans. Research Center*

ACKNOWLEDGEMENTS

Several groups and individuals contributed to the success of this project, to whom the present author is extremely grateful. In particular, Dr. Liuxi Tan, Co-PI, of this project, at Center for Advanced Microstructures and Devices (CAMD) at Louisiana State University (LSU). He was the principal force behind the system design, sensor testing and programming. The IDEA (Innovation Deserving Exploratory Analysis Programs) Project Manager, Dr. Inam Jawed, must be specially thanked for being always available for guidance and help. The author also thanks Harold "Skip" Paul, Director of Louisiana Transportation Research Center (LTRC), Dr. Zhongjie "Doc" Zhang and staff from LTRC for invaluable help on laboratory and field testing of sensor platform.

TABLE OF CONTENTS

ACKNOWLEDGEMENTS 1
EXECUTIVE SUMMARY 3
INTRODUCTION 3
CONCEPT AND INNOVATION 5
PROJECT PAYOFF POTENTIAL..... 5
TECHNIQUE OBJECTIVES 6
INVESTIGATION 7
- **Sensor Platform Design and Structural Layout** 7
- **Specifications of the Major Sensor Platform Components** 8
- **RF Transmitting/Receiving** 11
- **Self-Alignment Apparatus Shell Design, Fabrication, and Testing Results**… 14
- **Vibration and Road Material Acceleration Measurement** 18
- **Strain Sensor Calibration and Measurement** 20
- **Moisture Sensors Calibration** 24
- **3D Accelerometer for Sensor and Structure Tilt Measurement** 24
- **Faraday Charging Devices** 25
- **Pressure Sensor Performance** 27

CONCLUSIONS 27
REFERENCES 28

EXECUTIVE SUMMARY

This research is to develop a radio frequency (RF) ***wireless embedded sensor platform*** for monitoring strain/stress/temperature/moisture changes inside the asphalt/soil/concrete structures. The sensor platform deployment will neither significantly change standard construction procedures, nor the properties or performance of the structure. The platform has the capability of self-aligning using gravity force during the deployment, measuring localized strain/stress values from defined directions, and changing temperature. A MicroElectroMechanical-System (MEMS) type power recharging device will transfer the mechanical vibration caused by traffic into electrical energy to power the integrated rechargeable batteries. The sensor platforms can be either precisely embedded at designated critical sites or randomly placed in the highway structures during the construction time for overall structure performance monitoring and traffic information collection, such as traffic flow, vehicle's loading, speed, and axial numbers, etc. The main potential impacts on the practice of the proposed innovation include:

1. Provide a breakthrough technology for nondestructive monitoring and evaluating the performance of highway infrastructures at relatively low cost;
2. Provide a reliable tool to continually and remotely monitor the static and dynamic responses of highway structures to different loading conditions;
3. Provide the comprehensive data for verifying current highway structure design models and guidelines;

Provide a major component of Road Weather Information System for live highway dynamic traffic flow mapping.

INTRODUCTION

Federal Highway Administration (FHWA) statistics indicate that more than $20 billion of federal funds have been spent annually for pavement improvements [1] and the money spent on road by federal, state, and local agencies reached $66.3 billion in 2005 [2]. Therefore, any improvement in the design, construction, and maintenance of highway infrastructure alone will result in tremendous cost savings that include manpower and natural resources. In this regard, the importance of stress and strain information in highway infrastructure cannot be overemphasized. For instance, increased pavement durability and performance can lead to significantly reduced life-cycle costs due to the longer service life and less traffic disruption. The new mechanistic-empirical (M-E) pavement design guide has been developed to facilitate this endeavor. This new M-E guide is based on mathematical modeling techniques by using experimental data from materials and some actual parameter changes in pavement structures under traffic loading situations. The applications of the new design guide can only be enhanced with the knowledge of actual stress and strain levels at various pavement layers, which provide confidence in the new M-E model.

Wired sensors have been the traditional technology applied in highway structure research for in-situ stress and strain measurement. Wireless strain/stress measurements of highway structures based on RF data transfer approach have attracted more and more attention. Recently, many prototypes of RF wireless data acquisition systems have been used to study the highway bridges and structures [1-5]. In those studies, the actual sensor units were mounted outside the structures, and the RF transistors were stand-alone devices located on the testing structures separately. MicrosStrain, Inc. provides the RF data link module and lets users transfer data from their own sensors but not a complete sensor system. Usually, their RF data link is powered by battery and cannot be recharged if embedded in the structure, which will only provide a total working time of about 8 hours. For their newly developed batteryless EmbedSense™ data link system, an induction coil has to be placed close to the link (usually within 1 inch) for power supply purposes, so it is not suitable for highway applications. It needs to be pointed out that all of their products are not packaged for watery and dusty environments and they are not suitable for highway structures. However, the communication protocol between the sensors from MicroStrain, Inc., or a similar one can be adopted and implemented into this proposed sensor system. The recent development in highway remote monitoring area was the project initiated by the New Hampshire's Department of Transportation, in conjunction with Plymouth State University. That project tried to solve a particularly troublesome problem: unpredictable road surface conditions as part of the Road Weather Information System (RWIS) [8, 9]. A system used in the project consisted of a surface sensing part and a buried component, which were fabricated by Surface Systems, Inc., in St. Louis, MO. This system was hardwired from a highway structure to a stand-by data collection control station, and the collected data was sent out from the control station to the transition tower by either RF or cable. All aforementioned studies have made great progresses on wireless data acquisition but still have significant drawbacks such as, incomparable embedding, complicated deploying procedure, difficult customizing, etc.

For this research, the proof-of-concept sensor platform is designed to measure the strain/stress in the vertical direction only and can be expanded in the future to measure multi-directional strain/stress if needed. It can be aligned by itself utilizing the gravity through a special designed shell apparatus to ensure that the stress/strain readings come from a defined direction. The RF wireless data management protocol will ensure the easy deployment, less interference, and convenient operation. Since the sensor platform has capability to harvest electrical power from the traffic induced vibration, it will have a longer service life.

The main specifications for the proof-of-concept sensor platform were set as the following: (1) the maximum pressure range is from 0-100 psi with the accuracy of 0.5 psi, (2) the RF data reader should have a dynamic response in the range of milliseconds with a signal to noise ratio higher than 3, and (3) the sensor control and data transfer will be realized vs. wireless protocol from nodes to the road side data managing station. During the sensor platform development, the commercially available components have been used in order to increase the

performance, functionality, and reliability. As general practice in the Information Technology (IT) industry, the whole RF unit has been customized and produced by an Original Equipment Manufacturer (OEM), which will result in smaller size, lower cost, and better platform for possible future commercial production.

Since the proposed sensor system can measure instant load and send it out by RF network from a pre-located position, it can be used to map dynamic traffic flow with the information regarding the vehicle's loading, speed, moving-pattern, vehicle-spacing, axle-count information, etc. These critical data can also be used to verify and validate the M-E design parameters and give highway design engineers the ability to implement the "First Level Design" approach of the M-E design guide. Furthermore, it may also function as a potential road-surface-condition indicator to signal that maintenance is needed for pavement ride ability by monitoring the pattern of traffic flow and structural parameter reading changes.

CONCEPT AND INNOVATION

This **integrated, scaleable, and embedded RF wireless highway sensor platform** can measure the real time localized material parameter changes during the traffic flow and true wireless protocol from sensor node to road side data collection station. It also can equip a built-in Faraday power harvesting devices transferring mechanical energy (vibration) from highway structures into electricity for powering the sensor. The sensor system can be deployed into highway structures during the construction period or maintenance time without significantly changing current construction procedures. For existing highway structures, the sensor can also be embedded either manually or randomly during the maintenance. Each sensor platform will monitor localized strain/stress/temperature/moisture parameters of the structures, which can be used in asphalt/soil/concrete materials without weakening the structure's mechanical strength and performance. The moisture level will be monitored by an integrated semiconductor hygrometer. By carefully integrating the readings from each sensor and networking them together, an overall status of traffic flow history, vehicle's information, loading condition, and the structure responding to traffic loading at pre-located position can be evaluated. Eash sensor platform can also be used as a digital tap by recording the information of construction parameters, maintenance history, environmental changes, and other related data to its on board memory, which can be written/read through the RF communication.

PROJECT PAYOFF POTENTIAL

One of the unique payoffs of this sensor system is to help the implementation of load and resistance factor design (LRFD) and rating of structures, especially the applications for critical highway structures, such as bridges and tunnels. Since LRFD need the inputs of load and resistance factors based on the actual measured variability of applied loads and internal stress and strain, the proposed sensor system will provide more accurate, more comprehensive data for the analysis. Considering the mandatory requirement that states must design all new bridges

according to the LRFD specifications began October 1, 2007, the beneficial impact of having such a sensor system available to highway design engineers and researchers will be much more significant. The platform can also be used as a comprehensive traffic-flow/structure-property/road-loading/environmental-change monitor. It will help highway administration master the road service conditions and plan ahead the as needed maintenance schedule.

TECHNICAL OBJECTIVES

The sensor system development includes four main components: (1) integrated-scaleable sensor body with MEMS based sensors, (2) customized RF sensor-control/data-acquisition circuit, (3) a MEMS made energy harvesting device to power the embedded sensor for sustainable operation, (4) sensor self-alignment/positioning apparatus that is used during random deployment period to ensure the sensor body toward a fixed orientation. For the proof-of-concept sensor, the objectives are:

(1) Stability: The sensor should be physically sound and durable in highway environment. It has been designed to operate from a temperature range from -58˚F to 212˚F.

(2) Localized measurements: The strain/stress/temperature values are measured from closely surrounding material, usually within a volume of less than 3 inch in diameter. Through the data ID, the exact position of the measurement can be tracked from the sensor mapping chart obtained during the sensor deployment.

(3) Adequate sensitivity and dynamic range: The stress sensor's sensitivity is higher than 0.1 psi. The integrated sensor system's sensitivity and the dynamic range will be better than 0.5 psi and cover a range from 0 to 100 psi, respectively.

(4) Well-defined force/strain measurement and their orientation: A proprietary self-aligned/positioning device has been used to position the embedded sensor during the deployment and ensure that the directions of measured forces are well defined.

(5) Wireless monitoring to eliminate wires and out-of-structure connections: Off-the-shelf RF components have been integrated into the sensor system with batteries and power harvesting components. A 433 MHz RF System-on-Chip IC has been specified for the first generation sensor system.

(6) Capability of accurate measurement: The commercial sensors have been integrated in the first generation sensor platform for reliable, accurate, strain/stress/temperature measurements.

(7) No perturbation to the structure and routine highway construction: Since the sensor system is small in size, about 3 inch in diameter for the first generation, it can go through 400ºF for a short period of time and has self-alignment/positioning mechanisms; the sensor deployment processes will be compatible to the current highway construction environment and standard procedures.

(8) Scalability: If more monitoring spots are needed, the extra sensor platform can easily be added to the desired locations. If more functionality is needed, then, more sensor elements can be integrated into the current platform with no need to change sensor platform physical design.

(9) Power harvesting function plus power conservation design for extended operation life: The whole sensor system uses a low power consumption design and integrates with a miniaturized Faraday battery charging device that will convert mechanical vibration energy caused by traffic into electrical energy of the rechargeable battery for an extended operation life span.

INVESTIGATION

Sensor Platform Design and Structural Layout

Sensor platform main frame is made from steel so it will have enough strength for using inside both asphalt and concrete structures without creating the week point. Fig. 1 is the layout design of the platform. The top half accommodates a double sided RF data acquisition/control/communication board as well as the pressure, strain, moisture, temperature, and three-axial acceleration sensors. The bottom half contains the rechargeable battery and Faraday energy harvesting devices. After the sensor assembly, the platform can be packaged with variety of materials, such as asphalt, concrete, clay, etc., according to the structure material, which will be embedded in (See Fig.2 for details). In this way, it will be guaranteed that the measuring data will accurately reflect the structure material's behavior. The packaged sensor platform has the center of mass at the bottom, which will make the platform behavior like a tumbler if it is not constrained. Then, the sensor platform will be packaged in the special designed self-alignment shell for the random deployment. When the sensor platform is randomly deployed during the construction time, the self-alignment shell will let sensor platform stay in the desired direction because of gravity. The shell will be crashed into small pieces during the compacting process and exposed the platform to the structure.

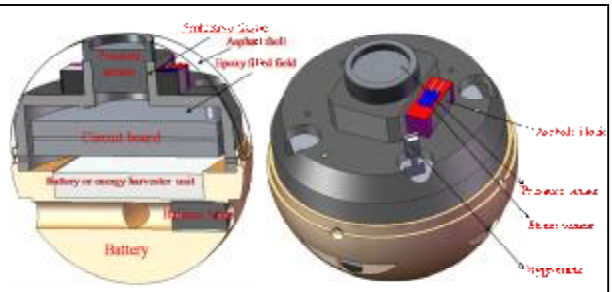

Fig. 1. The schematic layout of current sensor platform design.

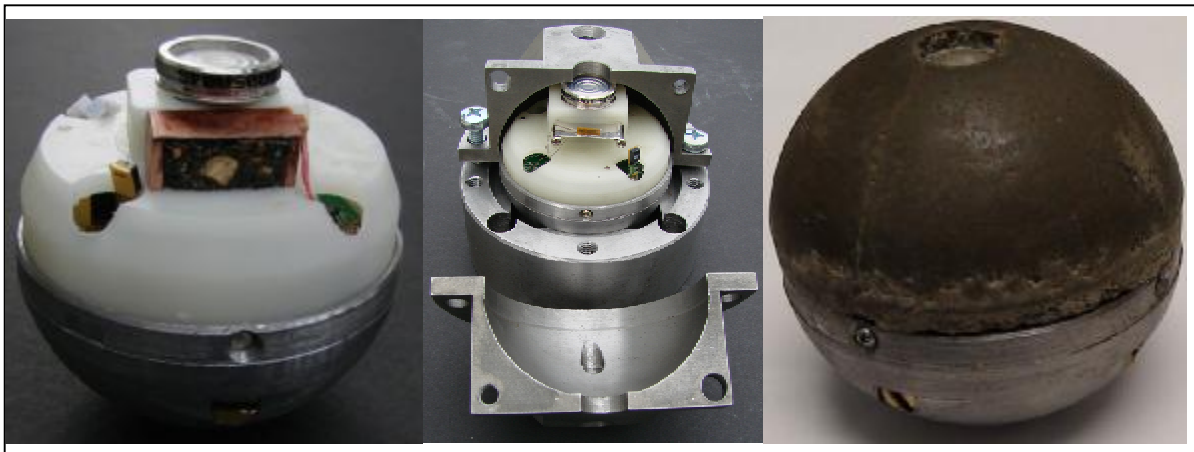

Fig. 2. Left is the assembled sensor platform, middle is the packaging apparatus, and the right is the sensor packaged with concrete used in the concrete structures.

Major Sensor Platform Components and Their Specifications

The pressure sensor. GE NPI-19 pressure sensor, as shown in Fig. 3, is currently chosen as basic pressure sensor platform for our project because it has a 8-bit Reduced Instruction Set Computer (RISC) processor, and a Low Frequency (LF) input stage to meet market demands for flexible, customer specific behavior/solutions, and overall system cost reduction. A programmable version of the sensor is also available for development purposes allowing researchers to download the application code in an electrically programmable ROM version. The detail information about NPI-19 is listed in Table. 1. A special sealer structure is added to the sensor surface in order to protect the sensor element from damage by intrusion of a hard

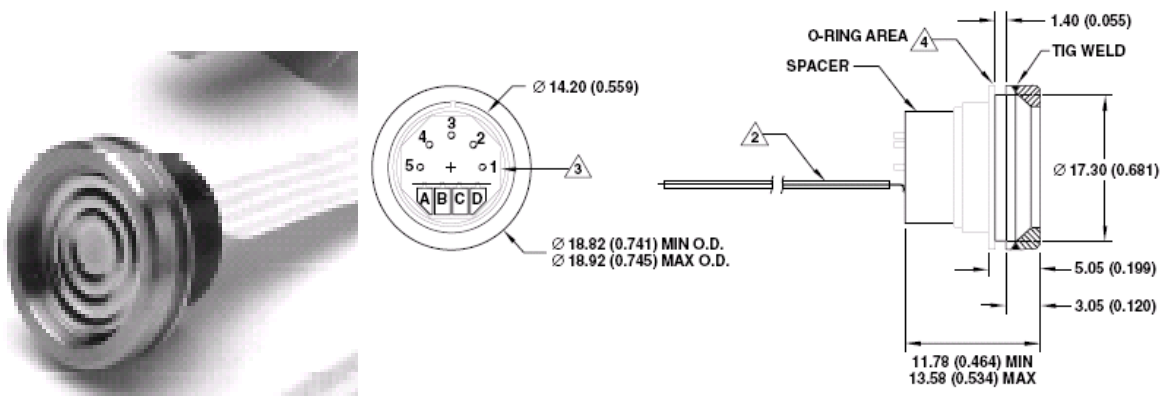

Fig. 3. The actually image (left) and schematic layout of GE NPT-19 medium range pressure sensor.

subject of the highway constructional materials. The sealer layer is designed in such the way that it will proportionally pass the outside pressure to the sensor and protect the pressure sensor's surface from damage at the same time.

Table. 1. Specifications of GE NPI-19 pressure sensor.

Parameter	Value	Units	Notes
General			
Pressure Range	0–100 0–200 0–700 0–1,700	kPa kPa kPa kPa	~0–15 psi ~0–30 psi ~0–100 psi ~0–250 psi
Maximum Overpressure	2X		rated pressure
Electrical @ 25°C (77°F) unless otherwise stated			
Input Excitation	1.0	mA	1.5mA max.
Insulation Resistance	10^8	Ω	@ 50 VDC
Input Impedance	4,000	Ω	± 20%
Output Impedance	5,000	Ω	± 20%
Bridge Impedance	5,000	Ω	± 20%
Environmental			
Temperature Range Operating(9) Compensated	 –40 to +125 0 to +70	 °C °C	 –40 to +257°F +32° to +158°F
Vibration	10	gRMS	20 to 2000Hz
Shock	100	g	11 milliseconds
Life (Dynamic Pressure Cycle)	1×10^6	cycles	
Mechanical(1)			
Weight	~10 ~45	grams grams	NPI-19A-XXX NPI-19B/H/J-XXX
Media Compatibility	All corrosive media compatible with 316 stainless steel		
Case and Diaphragm Material	316 stainless steel		
Recommended O-Ring	Type A: 16.76 dia. X 0.99 (0.66 x 0.039) Type B: 2-013 per ISO 3601/1		

http://www.gesensing.com/products/npi_19m_series_datasheet.htm?bc=bc_novasensor

The Microcontroller unit (MCU). Silicon Labs C8051F530 MCU is chosen for the system control, which is fully integrated, has low power consumption, and has a mixed-signal with a system-on-a-chip. Its function diagram is shown in Fig. 4, which has high-speed pipelined 8051-compatible microcontroller core (up to 25 MIPS) and true 12-bit 200 ksps ADC with analog multiplexer and up to 16 analog inputs. It owns precision programmable 24.5 MHz internal oscillator that is ±0.5% across voltage and temperature. It has 256 bytes of on-chip RAM to store all the program software. Up to 16 ports I/O and enhanced SPI serial interfaces make the system easy to integrate all the sensors in hardware. According to Silicon Labs' specification, the C8011F530 is a truly standalone system-on-a-chip solution, which has an on-chip power-on reset, a V_{DD} monitor, a watchdog timer, and a clock oscillator. The flash memory is byte

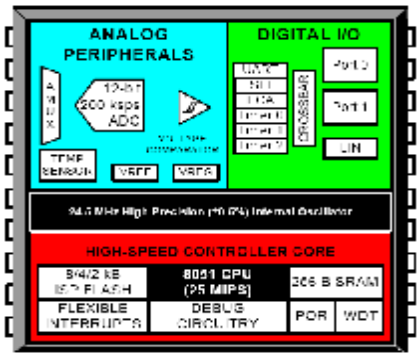

Fig. 4. MCU C8051F530 function block diagram.

writable and can be reprogrammed in-circuit, providing non-volatile data storage, and allowing field upgrades of the 8051 firmware. User software has complete control of all peripherals, and may individually shut down any or all peripherals for power saving. The on-chip Silicon Labs 2-wire development interface allows non-intrusive, full speed, and in-circuit debugging using the production MCU installed in the final application. This debug logic supports inspection and modification of memory and registers, setting breakpoints, single stepping, and run/halt commands.

RAMTRON FM3130 RTC/Alarm, an extra 64 Kb capacity non-volatility FRAM with real-time clock (RTC), is integrated as a flash memory for using as a digital tag to record the construction, materials, and maintenance information. Its function block diagram is shown in Fig. 5. FM3101 can be organized as two logical devices, the FRAM memory and the RTC/alarm. From the system perspective, they appear to be two separate devices with unique IDs on the serial bus. The memory is organized as a stand-alone two-wire nonvolatile memory with a standard device ID value. The real-time clock and alarm are accessed with a separate two-wire device ID. This allows clock/calendar data to be read while maintaining the most recently used memory address. The clock and alarm are controlled by 15 special function registers. The registers are maintained by the power source on the V_{BAK} pin, allowing them to operate from battery or backup capacitor power when V_{DD} drops below a set threshold.

The hygrometer. SENSIRION SHT75 hygrometer has been used in the sensor system for the moisture measurement. Its specifications list in Table 2. Since the hygrometer has an integrated temperature sensor, it can be used to measure road surface moisture and temperature simultaneously. The measured relationship between the surface moisture and temperature changes can be used to interpret road surface wetting and icing conditions, which are the critical parameters for highway management as well as engineers for traffic control, structure design, and maintenance schedule.

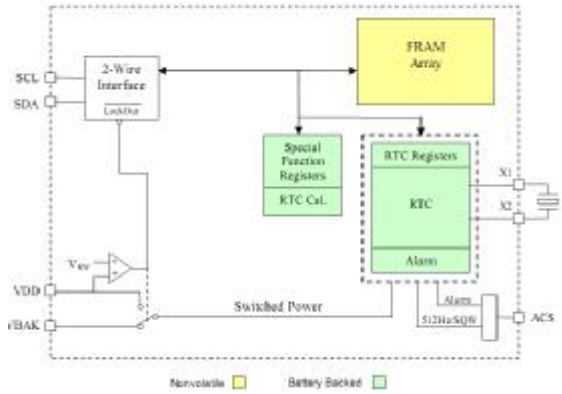

Fig. 5 . The function block diagram of FM3130.

Table. 2. SHT75 hygrometer specifications

Parameter	Conditions	Min.	Typ.	Max.	Units
Humidity					
Resolution		0.5	0.03	0.03	%RH
		8	12	12	bit
Repeatability			±0.1		%RH
Accuracy Uncertainty	linearized	see figure 1			
Interchangeability		Fully interchangeable			
Nonlinearity	raw data		±3		%RH
	linearized		<<1		%RH
Range		0		100	%RH
Response time	1/e (63%) at 25°C, 1m/s air	6	8	10	s
Hysteresis			±1		%RH
Long term stability	typical		< 0.5		%RH/yr

The strain sensor. OMEGA SDG-7/100 strain gauge is used to measure the strain changes of the materials. The highlights of this strain gauge are: 1-axis linear performance with accurate and fast response for static and dynamic applications, small bending radius with broad temperature range, and easy accessible solder pads/wire lead connections, and clear alignment marks for easy implementation.

RF transmitting/receiving

ATMEL ATA5823 highly integrated UHF ASK/FSK multi-channel half-duplex and full-duplex transceiver with low power consumption has been used for sensor platform data RF communication. The working frequency range is 313 MHz-316 MHz. The data rate is 1-20 Kbit/s using frequency-shift keying (FSK) or 1-10 Kbit/s using amplitude-shift keying (AFK). The system block diagram of ATA5823 is shown in Fig. 6. According to the manufacture, the ATA5823 is fully integrated, very low supply current, high sensitivity, and data transfer rate RF chip. Other highlighted features are listed below.

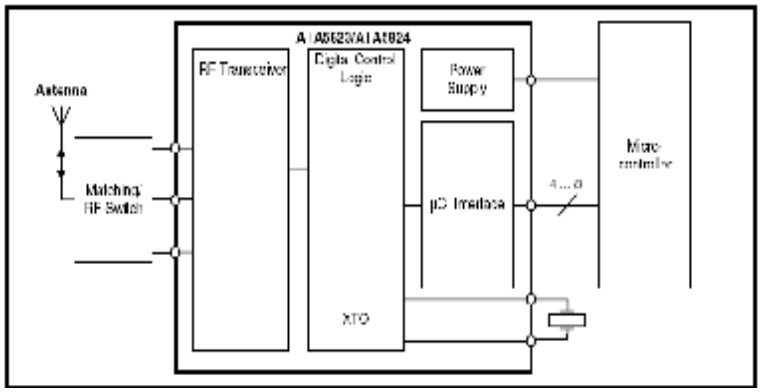

Fig. 6. System block diagram of ATA5823.

(1) Full duplex operation mode without duplex frequency offset to prevent the relay attack against passive entry go system
(2) High sensitivity: -105 dbm at 20 kbits/s/-109 dBm at 2.4 kbit/s (433.93 MHz)
(3) Low supply current: 10.5 mA in RX and TX mode
(4) RSSI-received signal strength indicator
(5) Integrated XTAl capacitor
(6) Fully integrated PLL with low phase noise VCO, PLL loop filter and full support of multi-channel operation with arbitrary channel distance due to fractional-N synthesizer
(7) 433.92 MHz, 868.3 MHz and 315 MHz capability without external VCO and PLL components
(8) Adjustable output power: 0 to 10 dBm adjusted and stabilized with external resistance
(9) Programmable output power with 0.5 dBm steps with internal resistance.
(10) Supply voltage range: 2.15 v to 3.6 v or 4.4 v to 5.25 v
(11) Temperature range: -40ºF to 302ºF
(12) Small 0.28 in X 0.28 in QFN48 package.

The RF data transfer and control circuits are customized into double-sided round-shape PCB. The standard RF power output is 10 dBm. In order to compensate the embedded environment, a power amplifier is integrated on the board to increase the total output power to 20 dBm to ensure the data retrieving even in extreme harsh situation. The flow charts of RF data acquisition and control are shown in Fig. 7. The system control protocol and diagram is shown in Fig. 8. The final OEM RF board is shown in Fig. 9.

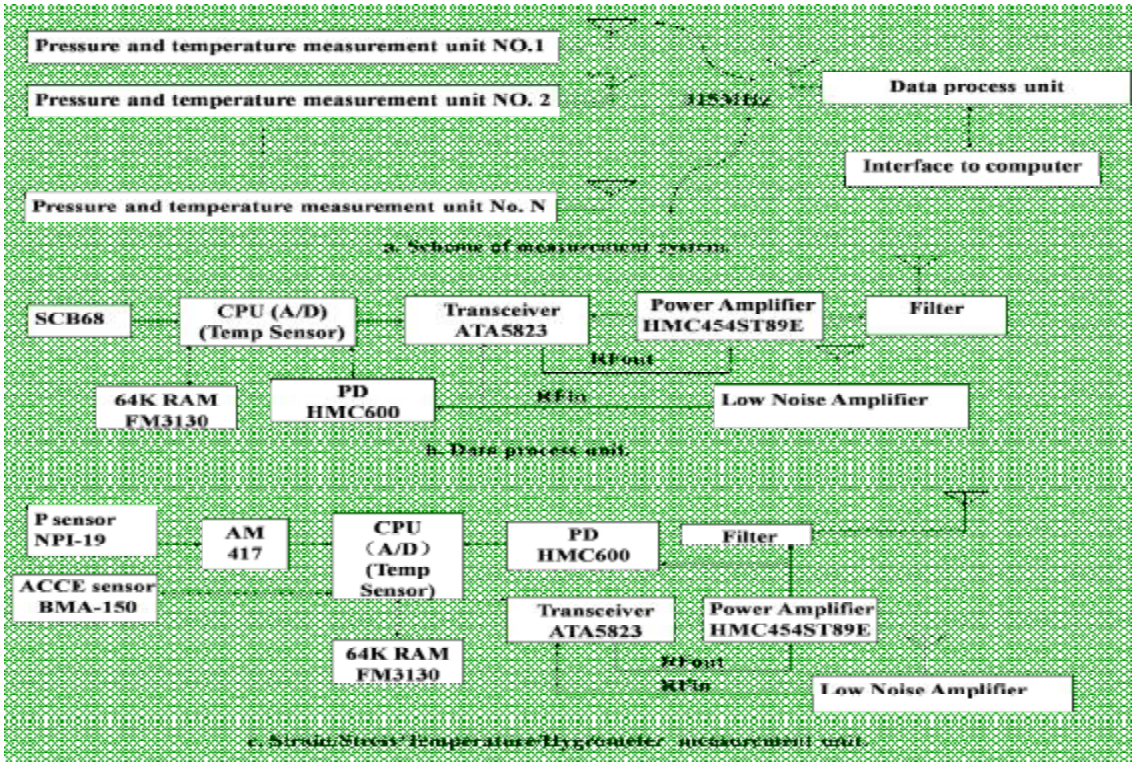

Fig. 7. The flow chart of RF data acquisition and control of sensor platform.

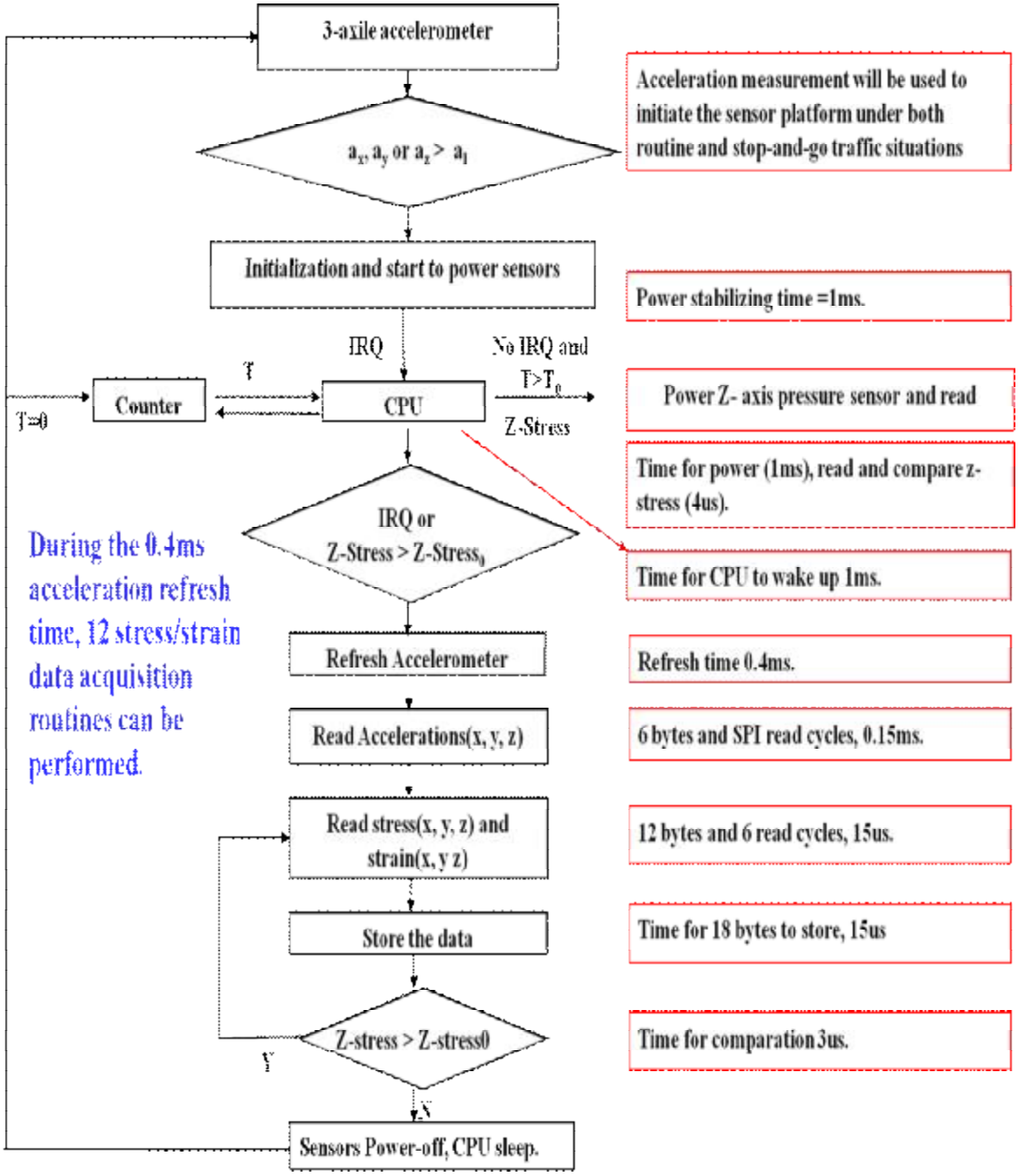

Fig. 8. The sensor platform control protocol and control diagram.

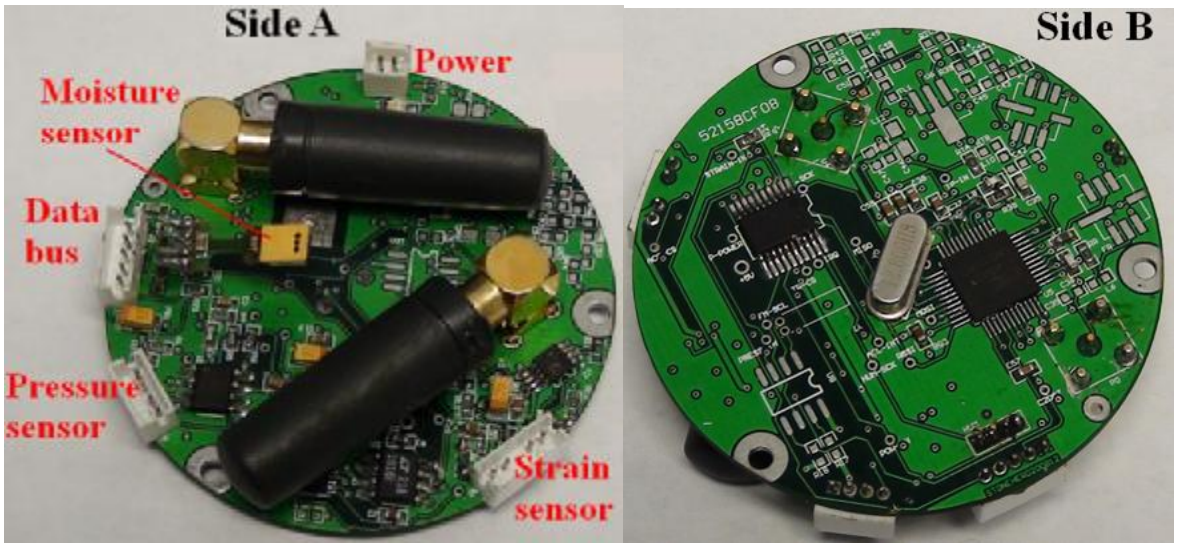

Fig. 9. The OEM double sided PCB for RF data acquisition and sensors control.

Self-Alignment Apparatus Shell Design, Fabrication, and Testing Results

The sensor platform alignment during the deployment is achieved by combing the sensor platform's tumbler behavior and a self-alignment apparatus, which is illustrated in Fig. 10. The apparatus is a hollow shell made from brittle ceramic or clay materials with an inner diameter a little bit larger than the ball shaped sensor platform. Since the platform behaves like a tumbler, it will stay in fixed orientation by gravity. The shell is designed in such a way that it is strong enough to undergo the mixing processes of asphalt/clay-soil, but it will crash into small pieces at the designed pressure. Therefore, the sensor platform can be thrown in the asphalt or other material during the mixing process, and then, align itself vertically during the material spreading. The shell will crash into small pieces at the pressure of compacting and let sensors expose to the environment while remaining in a near vertical position. Any small amount of tilting because of following compacting processes will be measured by integrated the three-axis acceleration sensor, which will give final orientation of the strain/stress directions at the accuracy of 1 degree.

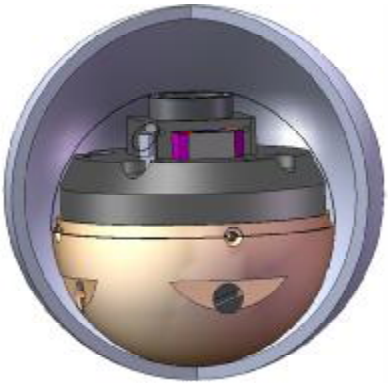

Fig. 10, The illustration of self-alignment apparatus assembly.

In order to design the proper shell structures, the stress/strain distributions inside the asphalt road and throughout the self-alignment shell during the compacting are essential. Since the stress/strain values introduced by the road roller during the compacting process decrease from the surface to the bottom of the road structure, PIs use the stress/strain at the depth of 0.5 m

(~2 ft.) for simulation study. The shell performing properly in this depth will function well when embedded depth is smaller than 0.5 m (~2 ft.).

Stress/Strain distribution during compacting processes. In the simulation processes, a four layers road structure is adapted and the detail information is shown in Fig. 11. In this situation, the maximum compression zone is about 6 in down from the road surface. The simulation boundary conditions for investigating the strength of the self-alignment shell are shown in Fig. 12. The maximum embedded depth of the sensor platform is 6 in beneath the road surface and inside the treated soil foundation layer.

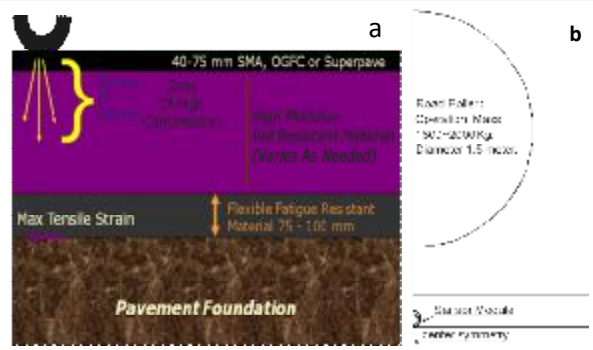

Fig. 11. a. diagram of a typical road structures; b. showing the model built for simulation.

Finite element model. The mesh of the whole model is obtained using software Hypermesh 8.0. The boundary conditions used in the simulation are:

I. Road roller's operation mass (M) is about 18000~2000 g. the roller's diameter (D) and width (W) are about 59 in and 93 in, respectively;

II. The road surface displacement (h) under compacting mass (M) is calculated from following equation:

$$M \cdot g = P \cdot S = P \cdot W \cdot L_{arc} \quad (1)$$

where

P- the pressure caused by operation mass; W-width of the roller's wheel; L_{arc}-contact length between road and roller's wheel; and g- acceleration of gravity.

Since the mass and dimensions of roller are known, the values of L_{arc} at different situations can be obtained by equation (1). Therefore, the displacement value (h) can be calculated by using simple geometric relationship.

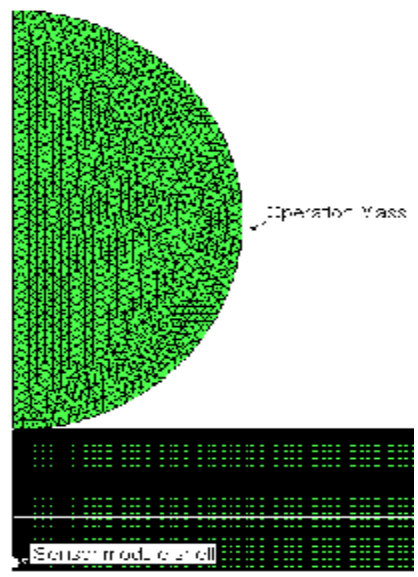

Fig. 12. Model of simulation.

III. The height of asphalt layer used here is 12 in and the sensor is 8 in inside the cement treated soil;

IV. The stress affected zone along the rolling direction is 12 in in front and 118 in after the roller contact point. The thickness of sensor alignment shell is 0.16 in;

V. The shell made from alumina based ceramic with elastic modulus of 300 GPa, flexural strength of 330 MPa, and compressive strength of 2100 MPa;

VI. The shell out diameter is 3.15 in with the shell thickness of 0.16 in (see Fig. 13);

VII. The groove dimensions are 0.04 in in width and 0.08 in in depth.

VIII. The range of h displacement on the road structure is from 0.787 in to 0.472 in.

The stress distribution around the roller's wheel and sensor are shown in Fig. 14. When the shell structure is intact, Von Mises stress distribution as the function of inner semicircle surface of self-alignment apparatus' shell with/without grooves are given in Fig15 and Fig.16, respectively. The results show that there is stress

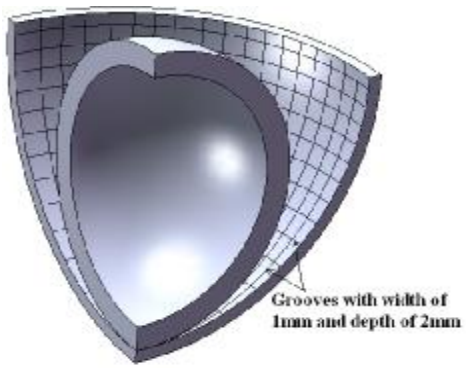

Fig.13. Illustration of self-alignment shell structure.

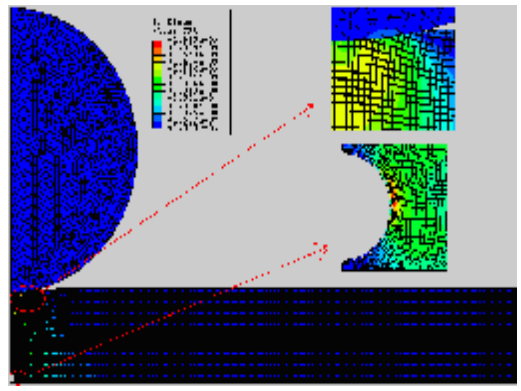

Fig.14. Stress distribution around roller wheel and sensor.

peaks at the top of the shell (0 in at the inner

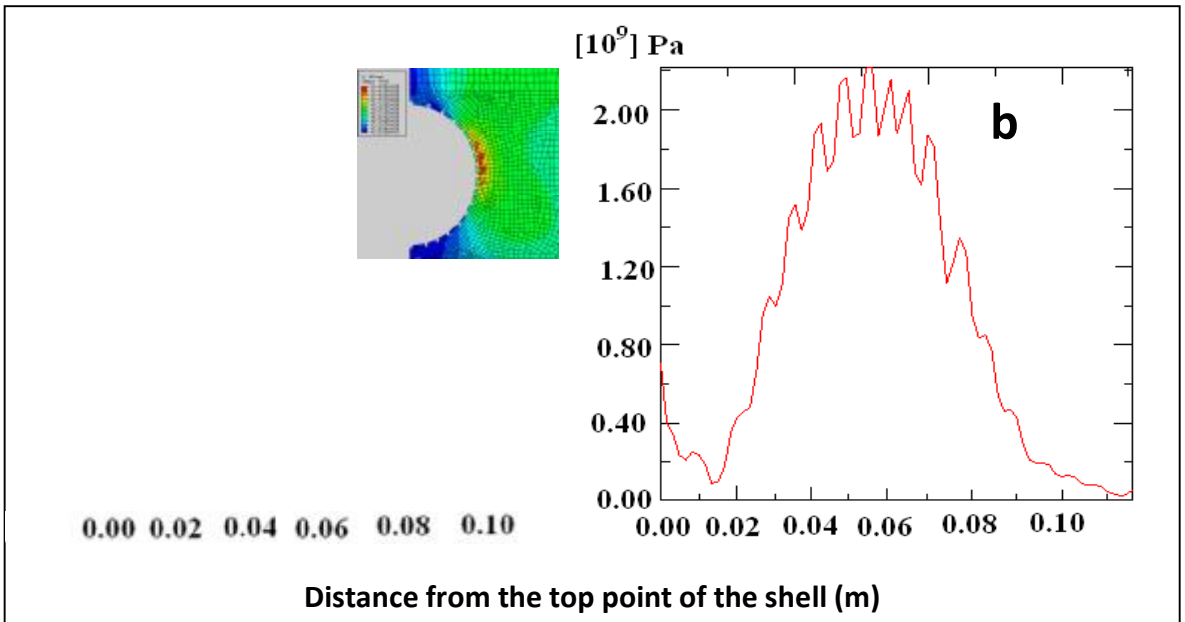

Fig.15. Von Mises stress distribution vs. the inner surface distance from the top point of the grooved shell structure when ***a.*** h=0.48 in and ***b.*** h=0.71 in.

semicircle coordinate) and the maximum stress at the position about 2.4 in from the top point. The groove structure has significantly increased the stress levels because of the stress concentration. The plots of stress along the radial direction vs. inner semicircle length for shell structures with grooves and different h values are illustrated in Figs. 15a & 15b. The results show

that the maximum tensile stress reached the flexural strength of the shell material at displacement of h equating to 0.47 in. For the shell structure without groove (Fig. 16), the maximum tensile stress under the same condition is only 150 MPa, which is far below the failure stress. According to the simulation, the grooved shell will first crack at the top. Once it fails from the top, the shell will no longer be a stable structure and the fracture will propagate from the top area to the whole shell because the stress concentration caused by grooves. The results indicate that the shell will be fractured during the compacting process, and it will eventually fracture into small pieces; therefore, the fractured shell debris will have a minimized interference with the stress/strain measurement of sensor platform.

A model assembly for making the grooved ceramic self-alignment shell has been fabricated using micro-sized electric discharge machining (EDM) according to the optimized simulation and design in Fig. 17. The self-alignment shells made from different ceramic materials are shown in Fig. 18.

The ceramic shells have been tested embedded in the sand with a confined space. The results show that once the stress reached the peak value of 1362 psi, the shell cracks along the grooves into many small pieces as designed (Fig. 19). This crashing stress value can be tuned according to different applications by change the ceramic material compositions and backing conditions.

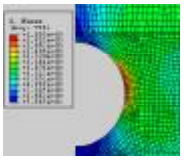

Distance (m)

Fig.16. stresses vs. the inner semicircle length of the alignment shell (h=12mm).

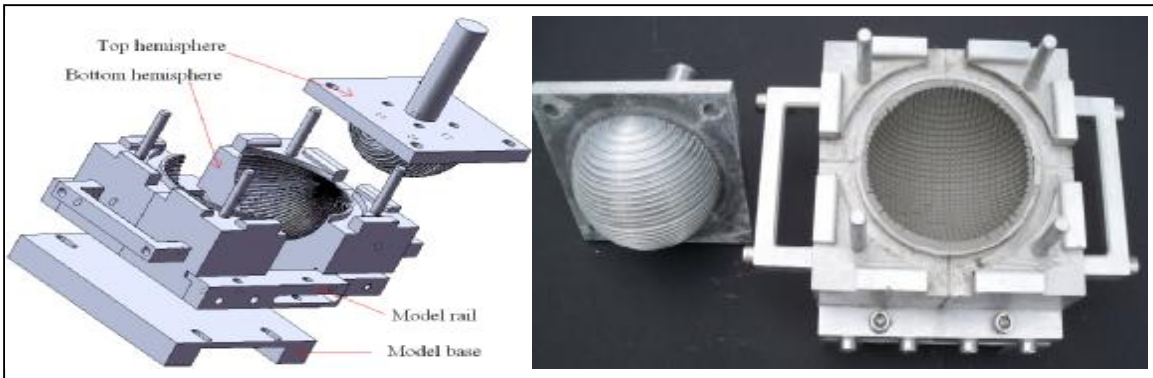

Fig. 17. The 3D drawing and the actually model assembly for making self-alignment shells.

The test results show that the designed self-alignment shell performed well for sensor platform alignment application. Besides the alignment function, the shell would also sustain the outside pressure, impact, and heat during the mixing and protect the sensor platform from high temperature damage and possible contamination.

Fig. 18. As made self-alignment shells with different type of ceramic materials.

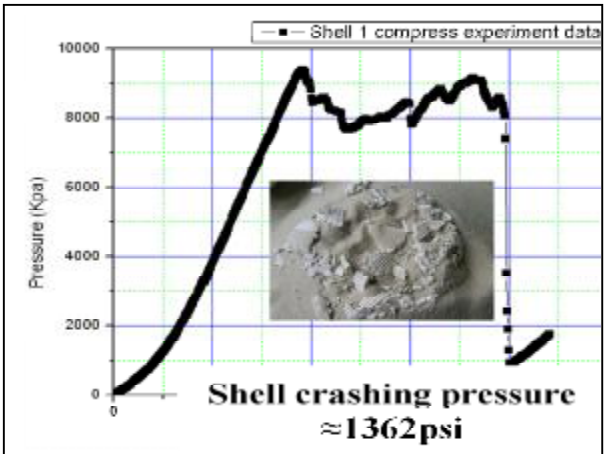

Fig. 19. The strength test results show that crashing pressure around 1362 Psi. The insert shows the shell is crashed into the small pieces.

Vibration and Road Structure Acceleration Measurement

Two sets of three axis-accelerometers have been embedded in and tested at road LA983. The purpose of this experiment was to collect acceleration information of asphalt structure along the X_Y_Z directions in the actual traffic flow and use the data to explore the possible applications of identifying the vehicle's axle number and speed. The general road vibration properties will also be used for energy harvesting devices design. Fig. 20 and Fig. 21 are the readings from 2 sets of embedded accelerometers at different embedded depths, which are 6 and 12 ins from the asphalt road surface for top and bottom sensor sets, respectively (as shown in Figs. 22 and 23). The results suggest that the acceleration velocity values are the function of the vehicles size and loading. The passenger can usually generates acceleration values from 0.05 to 0.25 m/s^2, and an 18 wheels can generates a $0.9 m/s^2$ of acceleration velocity. The highest acceleration value is in the vertical direction and two other orthogonal directions are smaller. The peak numbers of acceleration velocity are promotional to the axial numbers of the vehicle, i.e., two for a passenger car and five for an 18 wheel. The accelerations measurement results in Figs. 20 and 21 also show that frequency induced by traffic ranged from 10Hz to 20Hz at the road with speed limit of 45 MPH.

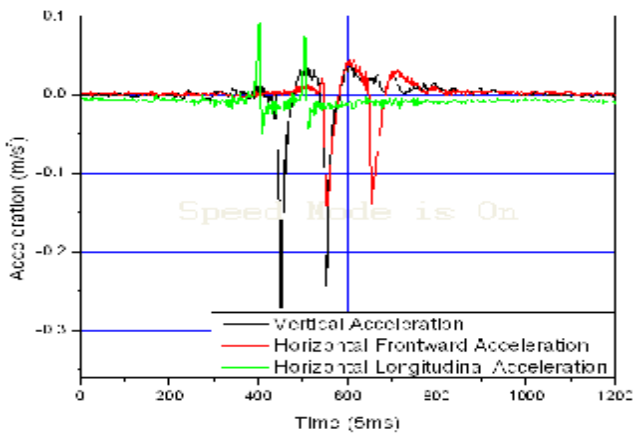

Fig. 20. Acceleration caused by a passenger car.

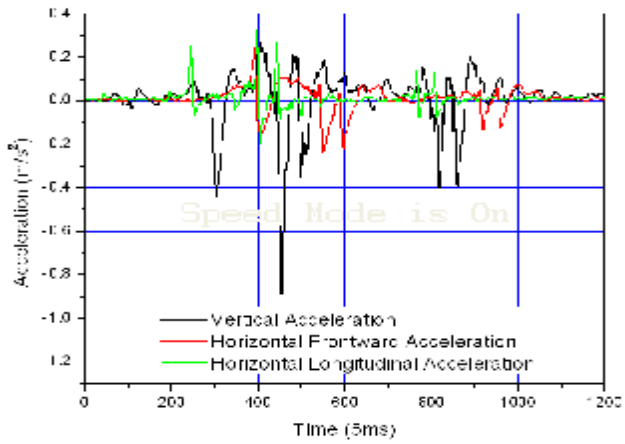

Fig. 21. Acceleration caused by an 18 wheels.

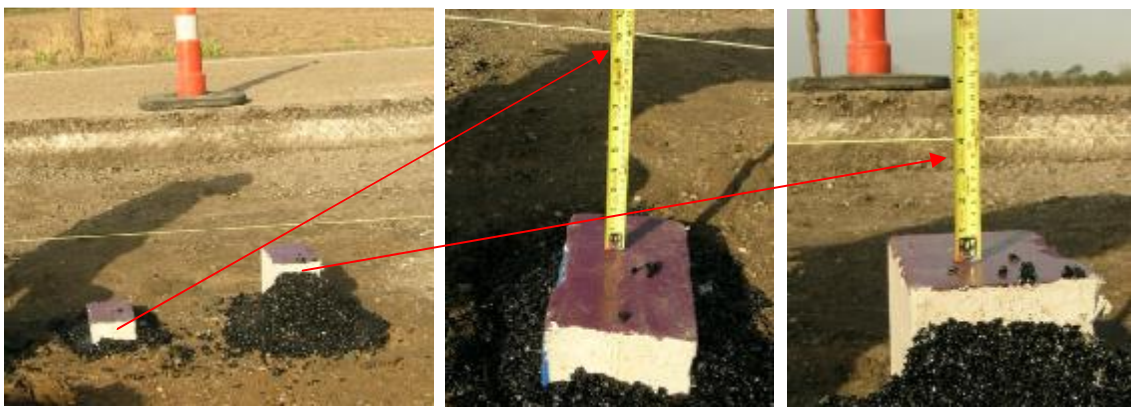

Fig. 22. Pictures show two accelerometers blocks have been placed in the LA983 for field test.

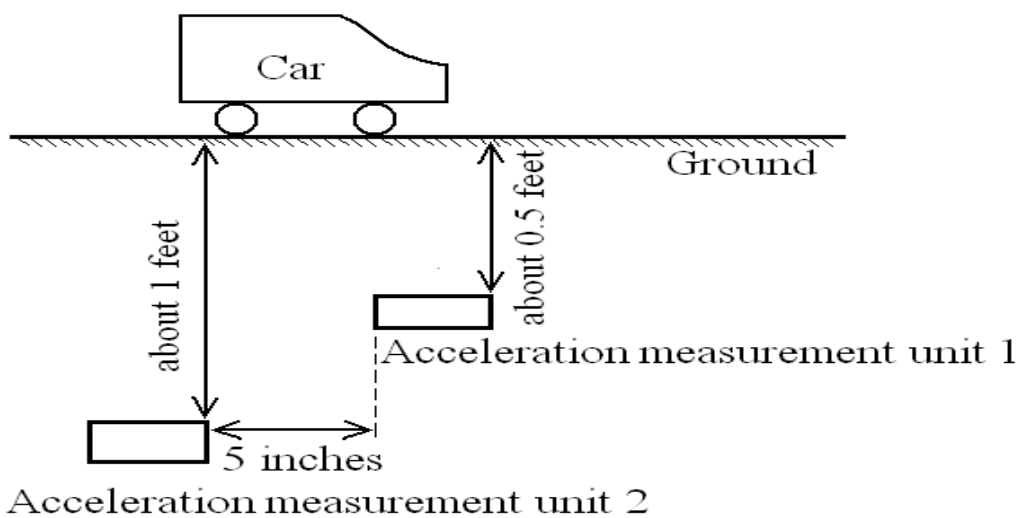

Fig. 23. Road vibration measurement illustration.

Strain Sensor Calibration and Measurement

Two kinds of embedded stain sensors have been calibrated inside the asphalt and cement materials at the Louisiana Transportation Research Center (LTRC). The temperature compensation strain gauges were placed on the top of the asphalt and cement blocks for measuring the actual strain values and eliminating the drift caused by temperature change. Fig. 24 shows the asphalt calibration setup and Figs. 25 and 26 are the calibration results. The strain sensors together with the RF control unit give a well-defined linear responses to the deformation of the asphalt block with the coefficient of determination (R^2) larger than 0.95.

Fig. 24. Setup for strain sensor calibration.

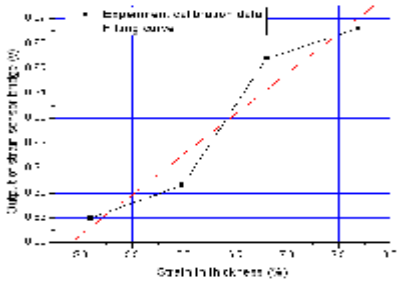

Fig. 25. Strain sensor #1 calibration results. the slope is 0.323and R^2=0.960.

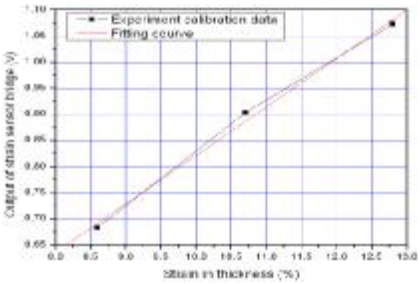

Fig. 26. Strain sensor #2 calibration results. the slope is 0.973and R^2=0.997.

Packaging the sensor platform in asphalt materials is the key process of this project. Among all sensor components, the strain gauge is the most sensitive component that may be damaged by the elevated temperature and excess stresses during the asphalt packaging process, Also, the original packaging materials on the rest of sensors and circuits are not designed to protect them from the elevated temperature and harsh environment such as hot asphalt. We have developed the proper procedure of applying protective material during the sensor platform packaging processes. The procedure of making asphalt packaged sensor platforms is illustrated in Fig. 27. The cement package procedure is much easier than the asphalt one. Simple cast process with a suitable model will accomplish the packaging.

The MTS 810 material testing system at Louisiana Transportation Research Center (LTRC) was used for the calibration processes and set up is shown in Fig. 28.

The loading used for calibration is a pulse force with different frequency values of 8, 12, and 16 Hz. The peak value of the load is 618 lb., which corresponds to 100 psi pressure in the tested sample (Fig. 29.). Asphalt packaged strain sensor was tested against the measurements from standard Asphalt Model Extensometer Model 3910. Figs. 30 and 31 show the results of the strain change measured by the extensometer and the developed embedded sensor platform, respectively. The results clearly show that the embedded sensor platform can accurately measure

the asphalt strain level as the function of the loading profile with the measure of the strain value matching the results obtained from commercial extensometer.

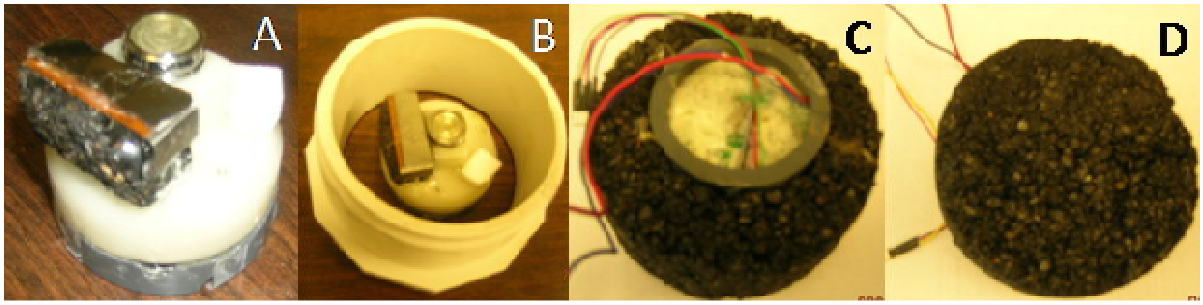

Fig. 27. Showing the prototype asphalt packaging process, (A) pre-packaging of strain gauge; (B) mold for sensor plat form packaging; (C) half packaged sensor platform; (D) The sensor platform fully embedded in asphalt.

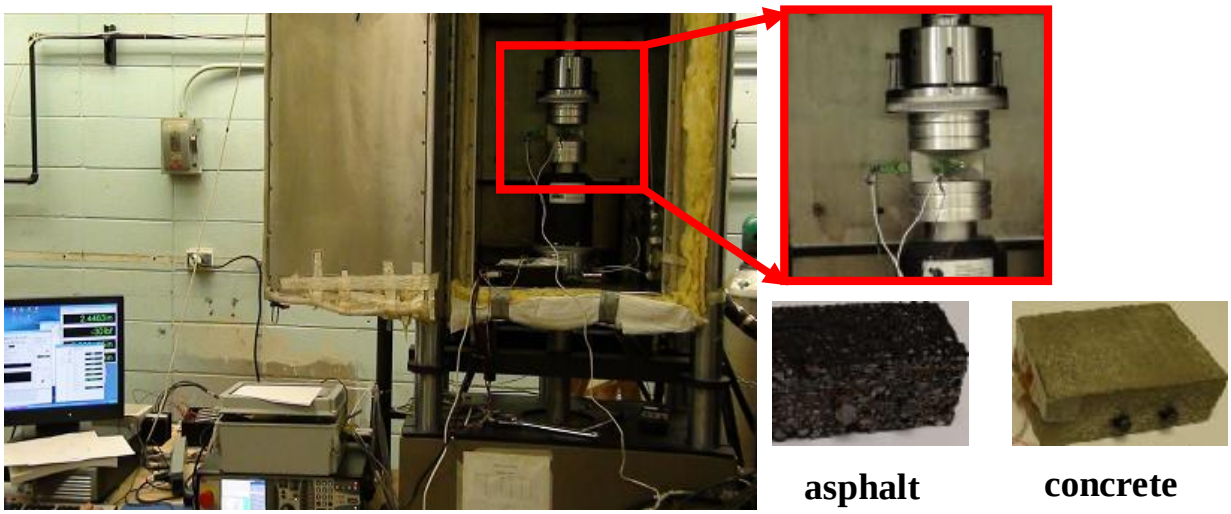

Fig. 28. The strain sensor calibration set up for asphalt and cement packaged strain sensors.

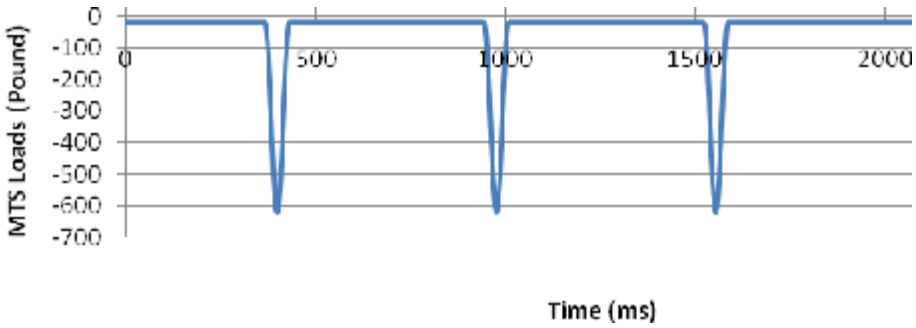

Fig. 29. The loading profile for calibrating the strain sensor embedded inside the asphalt.

It is generally recognized that the measured strain values of asphalt under dynamic loadings are the function of loading frequency. As the loading frequency increases, the maximum strain

value decreases for the asphalt material. This phenomenon is clearly demonstrated by measured results obtained from both the commercial extensometer and newly developed embedded sensor platform. The results show that developed embedded sensor platforms meet the asphalt strain measurement requirements with enough sensitivities on both strain level and responsive time.

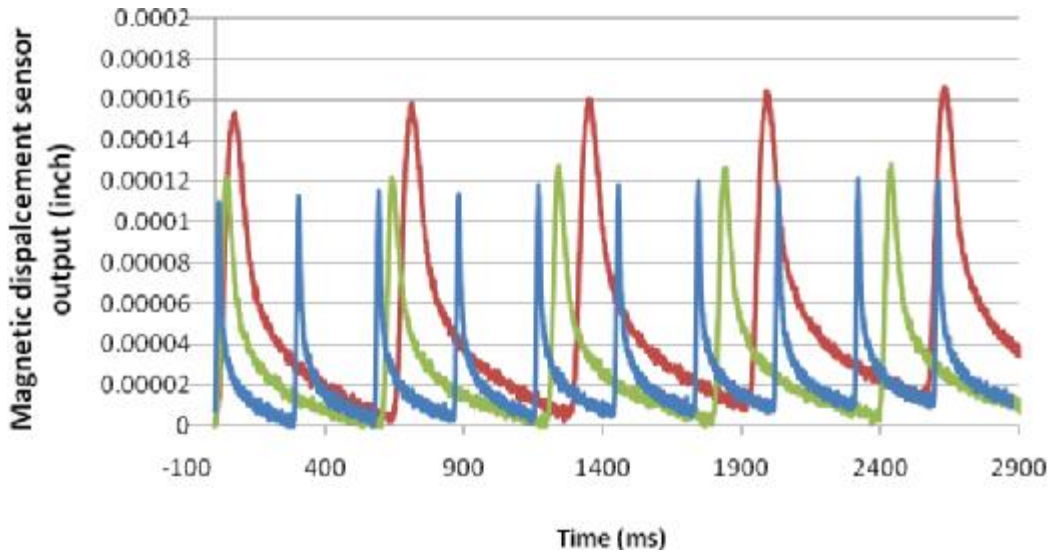

Fig. 30. Asphalt strain measurement results from Asphalt Model Extensometer Model 3910.

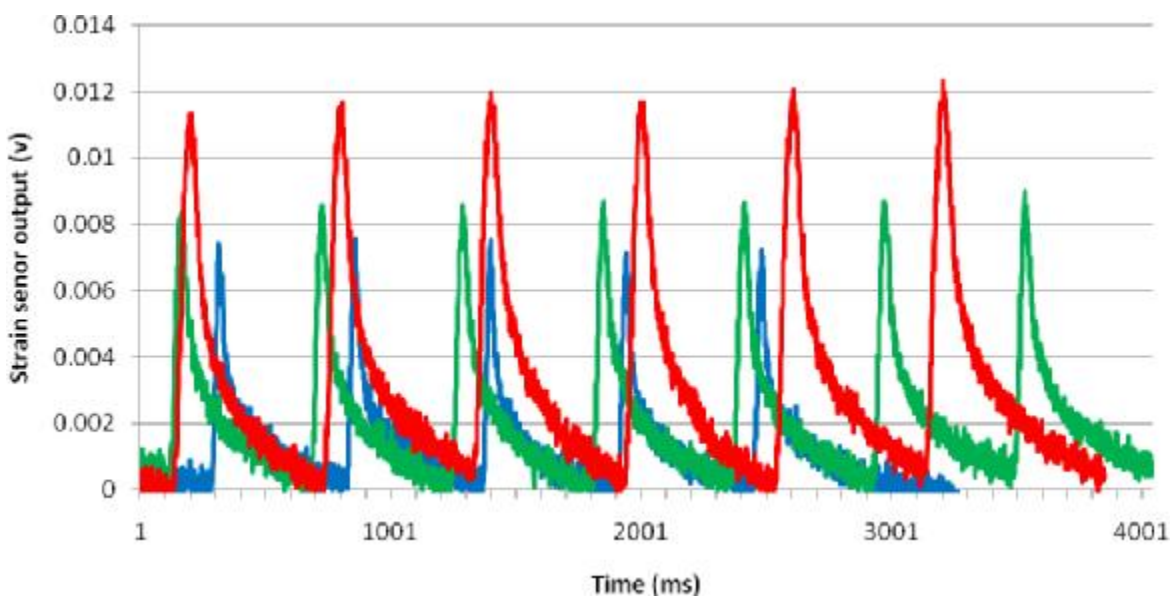

Fig. 31. Asphalt strain measurement results from developed embedded strain sensor.

The similar strain calibration tests also performed for the concrete material. The loading profile is shown in Fig. 32 with the maximum loading of 2000 lb (180 psi). The results also show that the embedded sensor platform has the same strain response behavior as the commercial extensometer, which suggests that the embedded sensor platform can reveal the true deformation behavior of concrete material under dynamic loading conditions (Figs. 33 and 34).

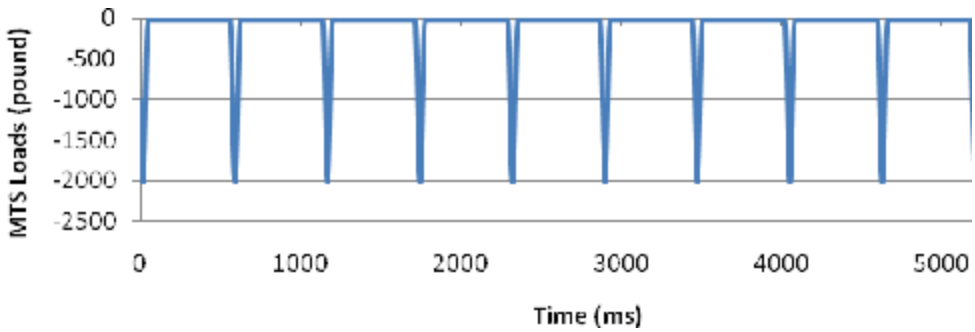

Fig. 32. The loading profile for calibrating the strain sensor embedded in concrete.

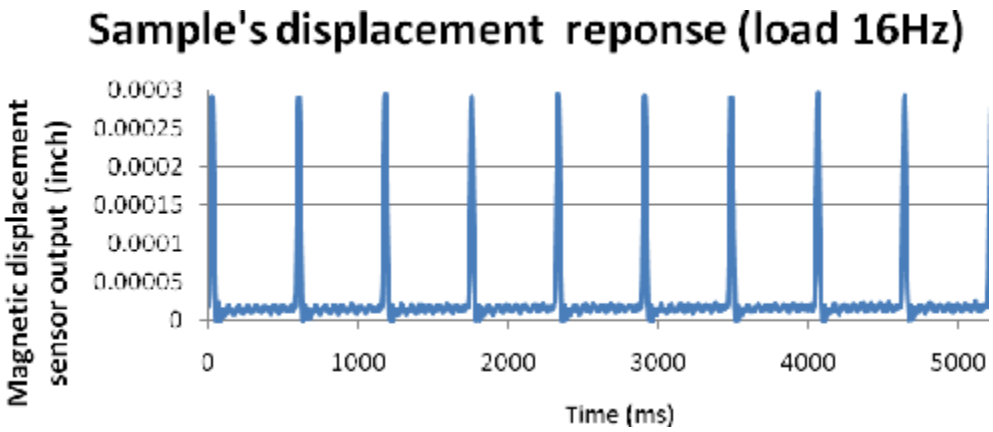

Fig. 33. Concrete strain measurement results from Asphalt Model Extensometer Model 3910 at loading frequency of 16 Hz.

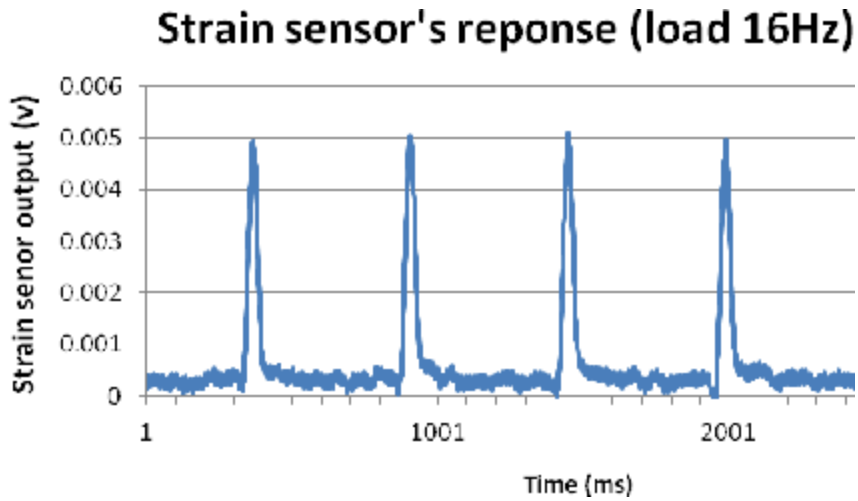

Fig. 34. Concrete strain measurement results from developed embedded strain sensor at loading frequency of 16 Hz.

Moisture Sensors Calibration

Moisture sensors used in the platform have also been tested against different water contents in the clay material. Two sets of tests with the duration of more than 20 days have been performed with the data collected at different equilibrium moisture conditions. The results show that with current moisture sensor, it only can measure the soil water content up to 1 wt%. If the water content is higher than wt1%, a different kind of moisture sensor has to be used. Fig. 35 shows the moisture calibration results.

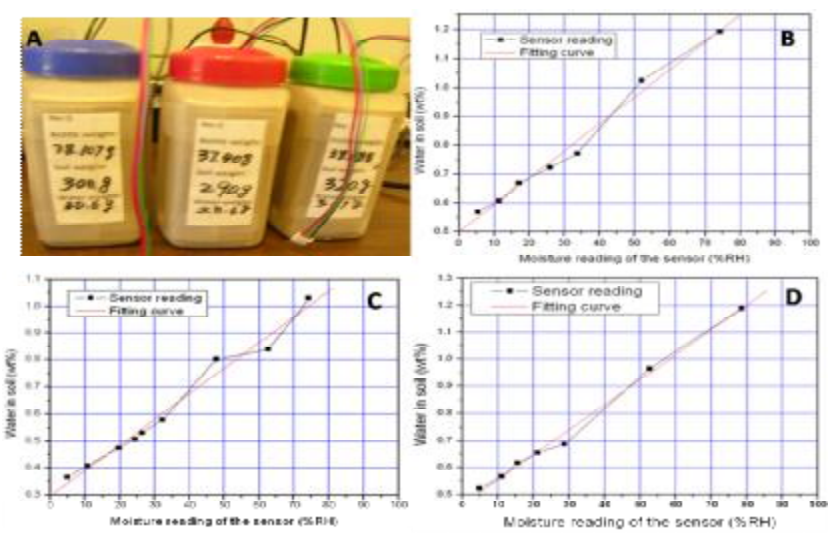

Fig. 35. Picture ***A*** shows the moisture calibration setup; ***B,C***, and ***D*** are the testing results from three moisture sensors. The average slop is 0.00935±0.00011 and R^2>0.99 for all.

3D Accelerometer for Sensor and Structure Tilt Measurement

The tilting sensor is based on the output of the Bosch three-axis analog accelerometer BMA140. The main problem to prevent the tilting sensor from proper performance in the developed sensor platform is the high frequency interference from environment (the noise above the 1 Hz). According to the factory specification, the frequency response of an accelerating readout can be expressed as equation (1), where $f_{C\text{-}X}$ represents the cutoff frequency of the

acceleration data of X-axis. Therefore, a proper RC low pass filter as show in Fig. 36 is added to filter out the interference of higher frequency noise. A 4.5 uF capacitor is used as Cx to allow a vibrating acceleration signal equal as or less than 1 Hz get to the A/D unit. In this way, the static gravity acceleration can be accurately measured and a 1° resolution can be achieved.

$$f_{c_x} = \frac{1}{2\pi * 33k\Omega * c_x} \quad (1)$$

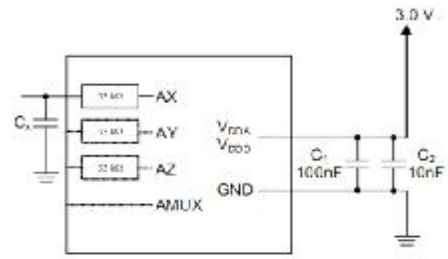

Fig. 36, Schematic illustration of the low pass filter for each axis.

A commercial accelerating data acquisition board and software from Bosch SensorTech are used to acquire the accelerating data from the developed sensor platform. The data with low pass filters is showing in Fig. 37. The outputs between two independent axes and their theoretical fitting from BMA140 are shown in Fig.38. Since the acceleration gradients from X, Y, and Z directions are orthogonal vectors, the sensor platform orientation in 3D space can be accurately determined once the X and Y vector values have been measured. The relationship between the tilting angles in X & Y directions can be expressed in equations 2 and 3.

X axis tilting angle (°):

$\alpha_x = \text{asin}[(0.2307*a_y-1.3493)*(a_x-0.35147)]$ (2)

Y axis tilting angle (°):

$\alpha_y = \text{asin}[(0.2662*a_x-1.3824)*(a_y-0.19134)]$ (3)

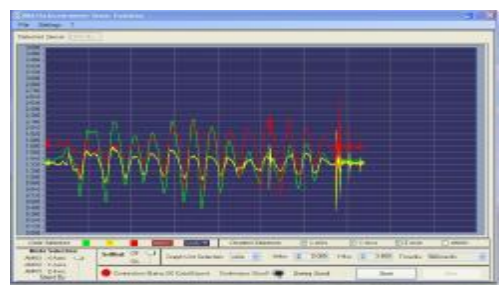

Fig. 37. Acquired accelerating data for all three axes with low pass filters.

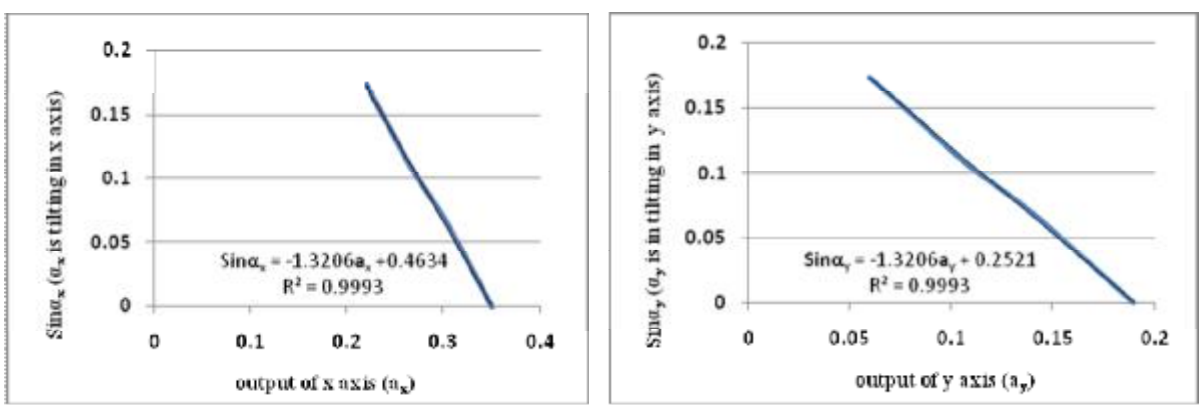

Fig. 38. Measured data from the X and Y axes show perfect match from theoretical match.

Besides the electrical noise filter, the mechanical environmental vibration noise isolator is also a key component to ensure the proper tilting reading with minimized interference. The

testing results (Fig. 38) show that accelerometer's output has a highly linear relationship as predicted after the installation of the low pass filter and environmental vibration noise isolator. The measurement accuracy meets the requirement proposed in the project—the accurate and repeatable measurement outputs with one degree resolution.

Faraday Charging Devices

One of the major power harvesting elements in the sensor platform is electromagnetic induction based device made from MicroElectroMechnical-System (MEMS) technology. The whole device design has been finished, finalized. The components have been under the fabrication and Fig. 39. show the assemble drawing of the device.

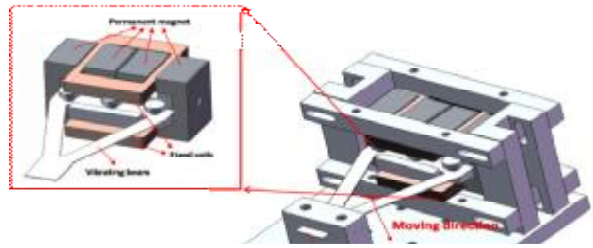

Fig. 39. Assembly drawing of electromagnetic energy harvesting device.

The U-shape permanent magnet is used in the device in order to provide the maximum magnetic field intensity at the opening gap. The magnet field intensity simulation results (Fig. 40) show that the magnetic field strength at 0.06 in opening would be 0.8 T when the permanent magnetic dimensions at the opening are 03 in in width, 01 in in height, and with cave of 0.31 in x 0.31 in.

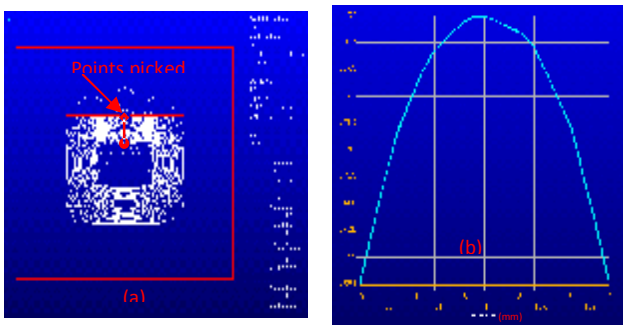

Fig. 40 (a) Simulation of the 2D magnet field intensity and (b) magnet field intensity at the points picked along line in the middle plane between U magnet ends.

The prototype of electromagnetic induction power harvesting device has been assembled and tested as a power source for the sensor platform. Fig. 41 shows the testing set up and the preliminary results of the electromagnetic induction power harvesting device. For the current designed Faraday device (small enough to fit the size of current sensor platform), the average power output is about 0.57 mW, which is not enough to power the current snsor platform (the sensor platform currently uses about 300 mW power). Therefore, the electromagnetic induction power harvesting alone cannot meet the power requirement and other compensation devices for power harvesting are needed overcome this shortcoming. One of the future solutions is to increase the size of the sensor platform to accommodate a large-sized higher power output Faraday device.

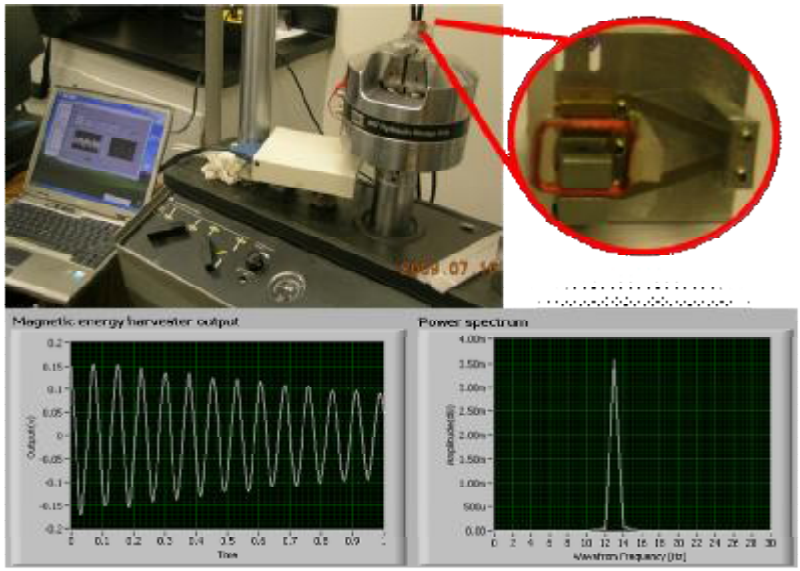

Fig. 41. Top picture is testing setup for energy harvesting experiment and the insertion shows detail configuration of electromagnetic energy harvesting device. The bottom figures are the testing results show that device resonance frequency is about 13 Hz and output is about 0.57mW .

Pressure Sensor Performance

The pressure/loading measuring experiments have been performed at LTRC using MTS materials testing machine with a loading range from 4 psi to 31 psi. Fig. 42 shows the actual pressure/loading measurement results. The overall system accuracy for pressure measurement is ± 0.1 psi. Because the packaging material caused a pressure offset, the pressure sensor has about 2 psi residue stress and can be easily offset from measurement software.

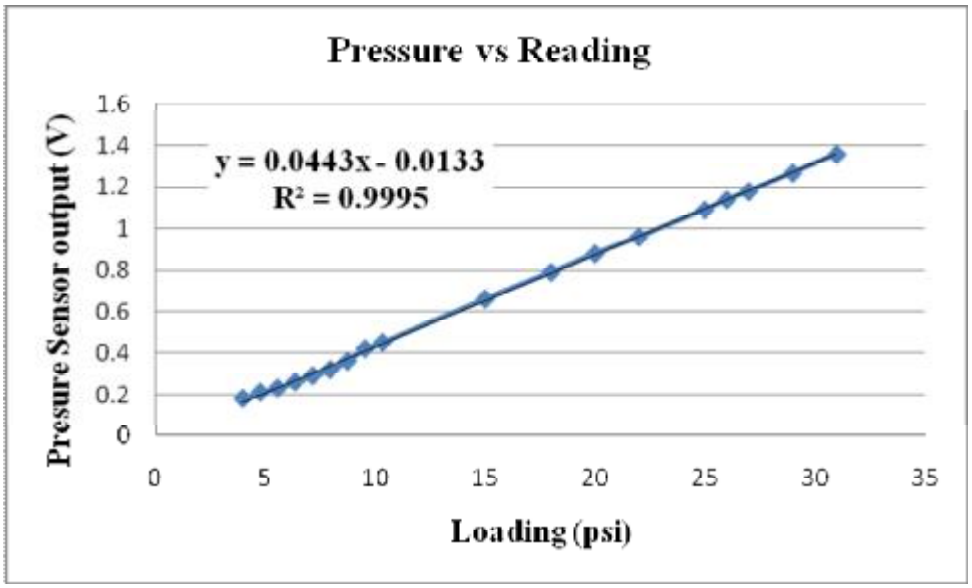

Fig. 42. The pressure/loading measuring results from packaged sensor platform, which show a linear performance with the $R^2 > 0.999$

CONCLUSIONS

The PIs have developed a sensor platform that meets all the proposed measurement criteria. It also has been demonstrated that with the increases of both platform size and power density the sustainable power supply may be achieved in the near future. The sensor platform can be deployed at a fixed orientation through the help of a self-alignment shell, which will save tremendous man-power and effort during the sensor platform installation. The developed sensor platform can measure the localized pressure, strain, moisture, temperature, accelerating vectors in x-y-z directions, as well as the structure tilting. The platform has a customized RF data acquisition/control circuits that can transfer data wirelessly while the sensor platform is embedded in the asphalt and cement structures. The platform demonstrated the capability of expending the functionalities as demanded. Because of the power consumption limitation, the RF data transfer range is currently limited within the range of less than 40 ft. Currently used moisture sensor can only measure the water concentration up to 1%w, which may be expended by changing the type of the moisture sensor. Because of the limitation of the prototype fabrication, the ICs and components in the RF circuits are soldered by hand, which is hard to ensure the high reliability. The preliminary testing results suggest that a fully automatic processing will solve this problem and ensure the reliability reach the current IC industrial standard.

The testing results also suggested that a developed sensor platform can be used not only to measure the materials property change caused by traffic flow and environmental changes, but also to detect the vehicle information, vehicle loading, traffic information, actual loading, and resulted material responses.

In summary, a prototype sensor platform has been developed through this IDEA program supported research. This platform shows the prospect futures for highway construction, maintenance, smart highway system, and instant traffic mapping applications. In order to commercialize the developed system, financial supports from federal, local governments as well as private sector are needed.

REFERENCES

[1] FHWA, "Design Guide Implementation Team(DGIT)," www.fhwa.dot.gov/Pavement/dgit/dgitfly.cfm

[2] Cauchon, D., " States Boostng Highway Spending," *USA TODAY*, December 5, 2005.

[3] Lynch, J.P., Wang, Y., Loh, K., Yi, J. H., Yun, C.B., "Wireless Structural Monitoring of the Geumdang Bridge Using Resolution Enhancing Signal Conditioning," *Proceeding of the 24th International Modal Analysis Conference (IMAC XXIV)*, St. Louis, MO, January 30-February 2, 2006.

[2] Pei, J.S., Kapoor, C., Graves-Abe, T.L., Sugeng, Y., Lynch, J. P., "Critical Design Parameters and Operating Conditions of Wireless Sensor Units for Structural Health Monitoring," *Proceeding of 42nd Allerton Conference on Communication*, Control, and Computing, Allerton, IL, Sep. 29-Oct. 1, 2004.

[3] Lynch, J.P., Partridge, A., Law, K. H., Kenny, T.W., Kiremidjian, A.S., Carryer, E., "Design of Piezoresistive MEMS-Based Accelerometer for Integration with Wireless Sensing Unit for Structural Monitoring," *Journal of Aerospace Engineering*, ASCE, July 2003, pp. 108-114.

[4] Lynch, J.P., "Detection of Structural Cracks Using Piezoelectric Active Sensors," *17th ASCE Engineering Mechanics Conference*, EM2004, June 13-16, 2004 University of Delaware, Newark, DE.

[7] Lynch, J.P., Sundararajan, A., Law, K. J., Kirmidjian, A.S., Carryer, E., Sohn, H., Farrar, C. R., "Field Validation of a Wireless Structural Monitoring System on the Alamosa Canyon Bridge," *SPIE's 10th Annual International Symposium on Smart Structures and Materials*, San Diego, CA, USA, March 2-6, 2003.